



Journal of Advanced Research in Fluid Mechanics and Thermal Sciences

Journal homepage:
https://semarakilmu.com.my/journals/index.php/fluid_mechanics_thermal_sciences/index
ISSN: 2289-7879



Thermal Variation on 18650 Cylindrical Cells under Different Testing Arrangement

Qurratul Haiqal Mohamad Rozi¹, Mohd Ibthisham Ardani^{2,*}, Mat Hussin Ab Talib¹, Muhammad Hanafi Md Sah¹, Madzlan Aziz³, Nursyafreena Atan³, Mohd Junaidi Aziz⁴, Fadhil Muslim Abd Oun Al-Dhalemi⁵

¹ Faculty of Mechanical Engineering, Universiti Teknologi Malaysia, 81310 Skudai, Johor, Malaysia

² UTM Center for Low Carbon Transport in Cooperation with Imperial College London (LoCARTIC), Universiti Teknologi Malaysia, 81310 Skudai, Johor, Malaysia

³ Faculty of Science, Universiti Teknologi Malaysia, 81310 Skudai, Johor, Malaysia

⁴ Faculty of Electrical Engineering, Universiti Teknologi Malaysia, 81310 Skudai, Johor, Malaysia

⁵ Iraqi Ministry of Electricity/General Company for Southern Electricity Distribution, Baghdad, Iraq

ARTICLE INFO

ABSTRACT

Article history:

Received 7 February 2024

Received in revised form 30 May 2024

Accepted 10 June 2024

Available online 30 June 2024

Keywords:

Lithium-ion battery; thermal non-uniformity; heat transfer

Cylindrical cell, especially with the 18650 format, is widely used for power electronics and electric vehicle. The cell's performance is strongly dictated by the current rate of charge/discharge and the cell temperature. The former is relatively easy to gauge because the value is constant for a certain period. Therefore, the cell performance can be mapped with respect to the current rate. However, the cell temperature varies temporally and dimensionally, making mapping cell performance concerning temperature difficult. This study employs a comprehensive thermal approach, with the aim to evaluate the degree of thermal variation with respect to various testing temperatures and cell arrangements conducted in a thermal chamber. Thermal measurements are measured, such as cell surface temperature at various cell locations. The experimental results provide an insight that different testing arrangements in which the cell is suspended vertically and horizontally do not alter the temperature variation of the cell significantly. Nevertheless, temperature difference up to 3°C is manifested along the cell surface, which happens at 5°C ambient temperature. This analysis highlights that cell temperature on the surface of 18650 cell is highly non-uniform, and the data could be further used to facilitate the cell's cooling system in for cells in this nature.

1. Introduction

Target graph data from the IEA Net Zero Scenario shows that the renewable generation of global electricity reached almost 29% in 2020, as described in the International Agency Report [1]. Since then, current energy has been chosen to be renewable energy and will be selected as the modern innovation towards green technology. Technological developments and electrification plans depend significantly on lithium-ion (Li-ion) batteries as this will drive other issue that stems from storage of

* Corresponding author.

E-mail address: ibthisham@utm.my

<https://doi.org/10.37934/arfmts.118.2.114127>

renewable energy as extensively described by Ardani *et al.*, [2]. Lithium-ion batteries have emerged as a preferred battery for the majority of electric vehicles mainly due to their high power density. This provides an advantage to run a high power brushless direct current motor, which greatly boosts speed, power, torque, and has a low maintenance requirement as described by Abd Aziz *et al.*, [3]. The responsiveness of battery installation enables emission reductions in the transportation industry, as highlighted by Richardson *et al.*, [4]. A cylindrical cell is one of the safest types of lithium-ion battery. It has good mechanical rigidity with built-in safety pressure vents, and the cell's manufacturing process is relatively mature. Therefore, the cell can be made at a higher capacity at a relatively lower cost as described by Deng [5]. In cylindrical cell design, a key concern, a short circuit, is minimized by putting foil strips of anode and cathode due to low internal resistance between them. The cylindrical cell design consists of an anode and cathode that roll around in the same direction in which the detail of design is explained by Wei *et al.*, [6]. Even though lithium-ion batteries have reasonable mechanical properties, they are also prone to thermal issues, especially during continuous charging and discharging, which significantly impacts lithium-ion battery life and performance, as described by Hunt *et al.*, [7]. To date, the cylindrical cell comes in variable sizes; the most common size is 18650. Other sizes are also available in the market, such as 21700 and 26500, with more storage capacity in large sizes. Typically, cylindrical cells have a capacity of 2Ah up to 4Ah per cell as mentioned by Wei *et al.*, [6] and Ouyang *et al.*, [8].

Some of the earliest research on lithium-ion batteries concerning battery performance under thermal gradient, low-temperature operation and thermal runaway was conducted by Spotnitz and Franklin [9]. Kong *et al.*, [10]. Subsequently, Hasan *et al.*, [11] and Troxler *et al.*, [12] conducted one of the most critical thermal analyses focused on thermal uniformity. The study highlights that thermal gradient across cell thickness affects the battery performance in which a high-temperature layer possesses a lower impedance. This causes larger currents to flow in this region. Additionally, Yang *et al.*, [13] and Huang *et al.*, [14] investigated the thermal gradient, including battery capacity variations regarding cell impedance variations. A battery with a thermal gradient has less operational capacity than its nominal capacity. On a larger scale, particularly battery modules, the impact of thermal gradient is much more pronounced, as described by Liu *et al.*, [15]. Wang *et al.*, [16] and Chen *et al.*, [17] expanded their research to explore the most effective thermal management method for lithium-ion batteries in a bid to improve the efficiency of battery performance based on temperature distribution using a simulation technique. This method is deemed necessary because some battery parameters cannot be directly measured. Therefore, this requires a robust computer simulation prediction to predict the battery's local SOC and internal temperature.

The temperature has a significant influence on battery performance. Therefore, much research is focused on the method for controlling the temperature of lithium-ion batteries, particularly for cylindrical cells. Battery thermal management (BTMS) is typically employed to gauge the temperature of cells in a module or pack to be within the desired temperature envelope. A basic system uses a phase change material (PCM) that wraps around the cell and absorbs heat generated by the battery, which is extensively described by Siddique *et al.*, [18]. A BTMS provides temperature control via two methods, which are active and passive. The active method requires a control system which can regulate the mass flow rate or the speed of the cooling medium. The cooling medium is typically in the form of air, liquid or a dedicated temperature control. A regulated pump is often used to control airflow to cool batteries in a pack or module. Higher air flow tends to keep the cell temperature relatively low. However, this will create a non-uniform temperature across the battery in the module/pack, as described by Wang *et al.*, [19]. On the other hand, liquid cooling offers better cooling capability; however, it needs comparatively higher power to pump liquid across the module/pack. Higher liquid viscosity will require more pumping power, as elaborated by Xin *et al.*, [20].

A direct cooling method via conduction is a more effective cooling system. However, this method is not suitable for use in actual operation due to its high power demand. This method uses a thermoelectric module to cool a surface to which batteries are attached. This method is employed by Troxler *et al.*, [12] and Lyu *et al.*, [21]. Additionally, Nasir *et al.*, [22] investigated the influence of heat through the piping method to stabilize the temperature within the batteries, which is reasonably practical in the BTMS system due to its simplicity and effectiveness in removing heat from batteries. Subsequently, Shetty *et al.*, [23] have used the BTMS system to optimize a liquid cooling system for a single cylindrical lithium-ion cell based on the modelling design of Newman, Tiedemann, Gu, and Kim (NTGK). The work presented uses a cylindrical cell with a diameter, which is essential because the heat generated will also increase as the cell gets larger in diameter.

On the other hand, the passive method is relatively simple. It depends solely on the external system of the battery in which the condition is relatively constant. Fan *et al.*, [24] evaluated the effectiveness of a phase change material. This method is acceptable if the current discharge rate of the battery is moderate. Nevertheless, due to the EVs relying on a more significant number of battery packs or battery modules, maintaining the temperature at the optimal battery performance is crucial, as described by Kumar and Goel [25]. Tian *et al.*, [26] conducted numerical research for a cooling system on a battery pack by using active control PCM. This is realized by placing PCM in an air duct. Therefore, the impact of active cooling can be achieved by regulating the air flow that passes through the PCM.

Wang *et al.*, [27] investigated the cooling impact of a battery pack using cylindrical cells to map the battery performance for cells with different consistency. It is found that force air cooling creates non-uniform cooling capability. Hence, higher cooling rates create larger cell performance variation. This finding is important, especially when dealing with cell placement in the module/pack. Yang *et al.*, [28] pointed out that the placement of the batteries is critical since an aligned arrangement of the battery will optimize temperature reduction. When force air cooling is used through a cylindrical lithium-ion module, the temperature differential falls by 50% compared to an unaligned battery configuration. There are several types of forced cooling. These include a U-type flow, as investigated by Lu and Tang [29], and a novel J-type flow, as investigated by Liu and Zhang [30]. The latter claimed that by designing a J-type cooling system, power consumption for the cooling system can be reduced by 30% while increasing the temperature differential by 70%.

Akbarzadeh *et al.*, [31] conducted computational research on the thermal analysis of a single 18650 lithium-ion cell cooling system. They discovered that the passive cooling approach is sufficient for the cell and the entire module at low current rates. The finding is essential to navigate away from over engineered design. Subsequently, Hong *et al.*, [32] released a study on a phase refrigerant of the typical cooler approach. This method can keep the surface temperature relatively constant. A relatively new cell matrix, the cell cooling coefficient (CCC), has been introduced. This gauges the cell's capability to reject heat depending on the cooling method and direction of heat transfer, which is extensively highlighted by Hales *et al.*, [33]. Therefore, due to the temperature being a vital aspect in achieving optimum cell performance and safety, it is essential to manage heat generation from the cell during usage, especially at higher current rates.

2. Methodology

2.1 Temperature Measurement Locations

An analysis of the variations in temperature's effects on cylindrical lithium-ion cells is deemed necessary to determine the extent to which thermal behaviour affects their capacity, power, and lifespan. Thermocouple detects temperature variation temporally; hence, thermal mapping on the

cell's surface can be obtained by placing several thermocouples in various locations along the cell surface. This is crucial as the cell undergoes an electrochemical process; it generates heat, eventually altering its performance due to temperature variations. In order to probe the temperature variations along the cell surface, high and variable discharge current rates are an effective method that will promote heat generation; therefore, significant temperature increases can be measured. The temperature measurement is conducted by securing thermocouples on the cell's surface using a kapton tape.

For this work, three thermocouples are attached to three different locations along the cell surfaces, as shown in Figure 1. The three locations are close to the cell's positive tab, centre, and negative tab, respectively. These locations were chosen mainly due to the appreciable differences in thermal resistance of the cylindrical cell. However, placing the thermocouple directly at both tabs is inherently challenging due to space constraints. Electrical connections at both tabs are required, which thoroughly wraps the tabs; hence, the thermocouples are placed slightly offset of both tabs, as shown in Figure 1. These locations could represent the average temperature at both tabs.

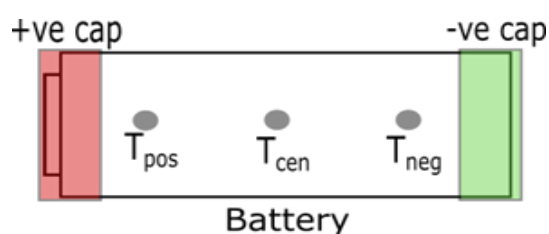


Fig. 1. Three thermocouple locations along the cylindrical cell (Near to positive tab, Centre and Near to negative tab)

As the temperature varies along the cylindrical surface, the thermocouples are positioned at three (3) locations: positive, centre, and negative, as illustrated in Figure 1. Two electrical connections are required, which are the connection to the positive and negative tab of the battery. The connection consists of a plastic holder with a metal terminal built on the inner side of the holder. This requires a bit of space at both ends to securely fix the holder. The thermocouples are attached to the cell's surface via Kapton tape. Subsequently, the cell is placed in a thermal chamber in which the thermal conditions exposed on the cell's surface are regulated from 5°C to 45°C with increments of 10°C.

As shown in Figure 2, two test positions are conducted to evaluate the possibility of thermal variation concerning cell position during the test. The cell is placed horizontally and vertically, with respect to the location of the thermal chamber fan. This primarily ensures that the further test result is independent of the cell's orientation. This initial comparison is crucial because heat transfer has a direction; therefore, minimising the impact of external heat transfer variation is essential to produce reliable findings.

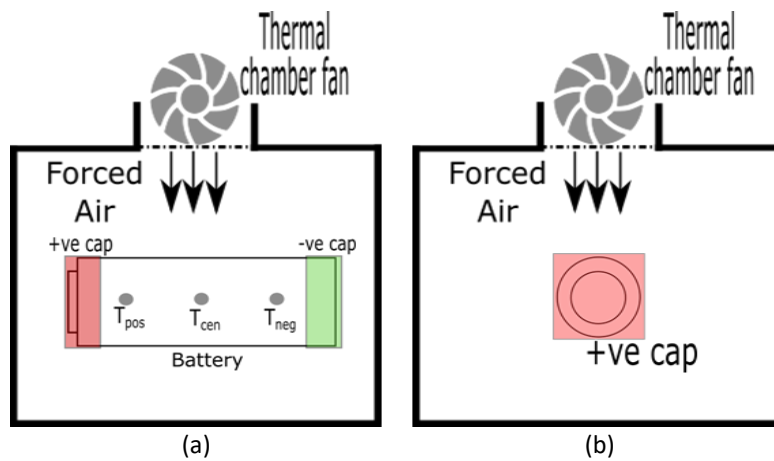


Fig. 2. Top view of cylindrical cell inside thermal chamber: (a) Cell is placed horizontal, (b) Cell is placed vertical

A thermal chamber is used to provide a different ambient temperature that artificially creates different external conditions for the cell. The thermal condition inside the chamber is regulated by a fan, which provides a forced convection condition on the cell surface. Prior to the discharge test, the cell is kept in the thermal chamber for at least 20 minutes. This allows the cell to reach thermal equilibrium at that test temperature before the discharging test is conducted. Once the test is finished, the chamber's temperature is switched to another test temperature. Subsequently, the cell is allowed to rest to allow for another thermal equilibrium at a new test temperature. This process is shown in Figure 3, whereby the chamber's ambient temperature is regulated from one test temperature to another.

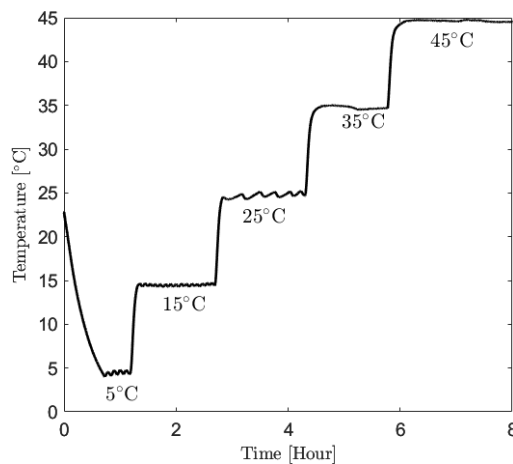


Fig. 3. Controlled ambient temperature at various test temperature

2.2 Battery Charging-Discharging System

The test utilises a pristine Panasonic NCR-18650B with a nominal capacity of 3.3Ah. Two electrical devices are used for the cell's electrical test, namely an electronic load and a power supply, as illustrated in Figure 4. The former is critical as the device provides a constant electrical load that discharges the cell at a specific current demand. On the other hand, the power supply provides a charging current to ensure the cell is at 100% state of charge (SOC) prior to discharging tests. BK Precision makes electrical equipment, and it uses dedicated software to switch between charge and

discharge. The system is unidirectional in that the current that passes from either the electronic load or power supply runs only in one direction depending on the set program and runs on a one-by-one basis.

Due to the arrangement of the electrical system, the cell needs to be connected in parallel. The cell's positive and negative tabs are attached to the electronic load and power supply separately, as shown in Figure 4. This eventually creates a parallel string between both systems. To ensure the cell is always at 100% SOC before the discharge test, a charging procedure which consists of constant current (CC) and constant voltage (CV) is conducted. The applied charging current is at 1C, which corresponds to 3.3A. This current is applied until the cell voltage reaches 4.2V. Subsequently, the charging mode switches to CV. This holds the voltage at 4.2V while allowing the current to drop until it reaches at least 500mA. A fully charged cell is defined when the current drops below 500mA during the CV charging and thermal equilibrium has been reached concerning the thermal chamber temperature.

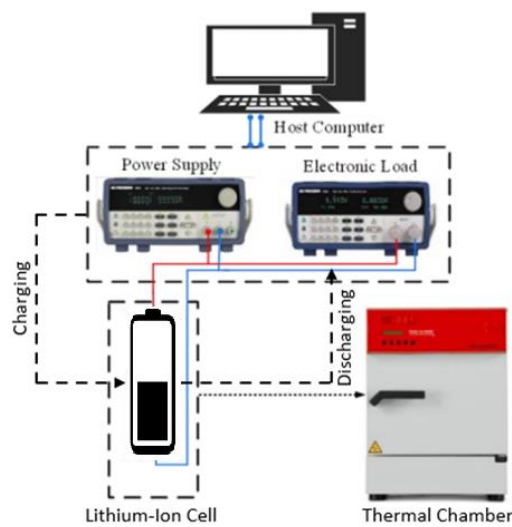


Fig. 4. Schematic of battery charging-discharging system

As mentioned, an initial test was conducted whereby the cell was placed horizontally and vertically. This aims to evaluate any differences in the cell's performance concerning the cell's test positioning. Figure 5 compares the cell's voltage curve at various test temperatures from 5°C to 45°C under a 2C discharge rate. It can be seen that the voltage curve from both cases is relatively similar. Therefore, a further test is conducted horizontally with the cell. For further analysis, discharge rates of 1C, 2C and 3C were conducted from this cell position. The voltage window for this cell is from 2.5V to 4.2V hence, the cell is charged and discharged only within this voltage window. These voltages correspond to 0% and 100% SOC.

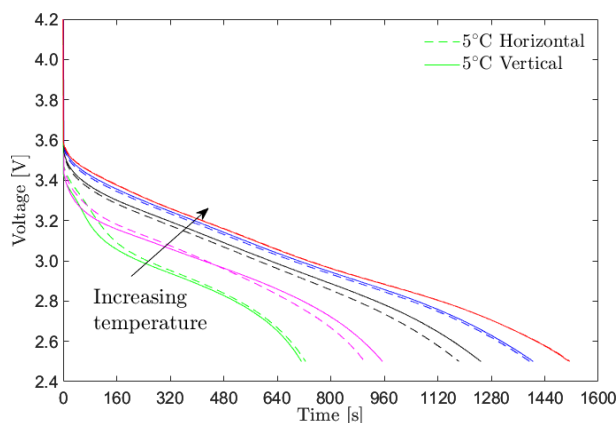


Fig. 5. Voltage curve comparison for horizontal and vertical arrangement (Dash line represents cell in horizontal and solid line in vertical position)

3. Battery Voltage Curve

Figure 6 highlights the behaviour of the voltage curve at three different C-rates and ambient temperatures. Since the cell is rated at 3.3Ah, the applied current discharges are 3.3A, 6.6A and 9.9A which corresponds to 1-C, 2-C and 3-C. When the cell is discharged at higher rates, it can be seen that the time taken for the cell to sweep from 100% to 0% SOC decreases. This is mainly because the energy from the cell is being taken at a higher power, causing rapid depletion of its energy content. However, although the variation of the discharge current applied is linear from low to high, the time the cell takes to reach 0% SOC, drops relatively exponential following Arrhenius's rate of law. The voltage curves have a distinct behaviour, especially at low discharge rates. Several peaks can be seen at along the voltage curve under 3.3A discharge, particularly at high ambient thermal conditions.

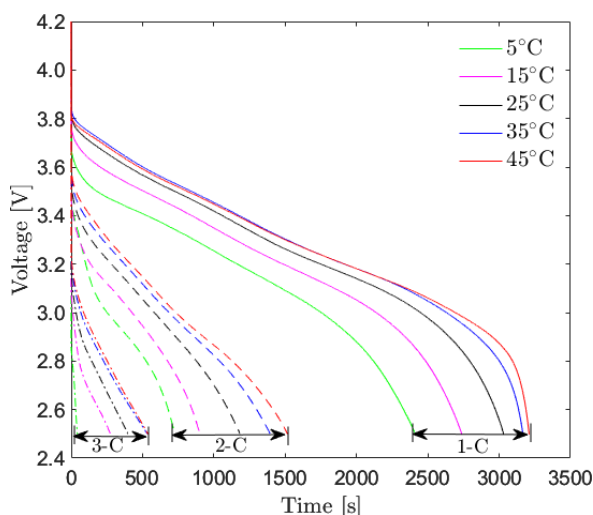


Fig. 6. Voltage curve at different ambient temperature and C-rate conducted at horizontal arrangement

Conversely, the voltage curve is relatively linear at a high discharge rate (2-C and 3-C), and this behaviour spans from 100% SOC to 0% SOC. The relatively linear trend of the voltage curve at high discharge currents contributes to the domination of irreversible heat. This eventually masks reversible heat during discharging and causes the voltage curve to be quite linear. The reversible heat

contains entropic relation which portrays the electrochemical behaviour of the cell, however the effect will not clearly appear in the event of high discharge rate. At high discharge rate, reversible heat in the form of joule heating dominates the heating of the cell.

The testing is conducted at a constant ambient temperature from low to high. Nevertheless, the test temperature is relatively narrow. This is primarily to prevent any significant cell degradation that could eventually affect the test data. No tests were conducted below 5°C or above 45°C. This aims to minimize the risk of degradation, namely lithium plating at low temperatures, and increase the cell's internal resistance at high temperatures. In relation to the ambient temperature effect, it can be seen that at all C-rates, the cell performs better at high ambient temperatures. The time it takes to reach 0% SOC is the longest in all cases for high ambient temperature testing. This happens due to a significant reduction of cell impedance at this temperature, which eventually reduces heat generation as current passes through the cell. The reduction in heat generation translates to more energy available to be used as a current output from the cell. On the contrary, testing at low temperatures results in relatively rapid cell depletion. A higher cell's impedance at this temperature generates more heat, eventually limiting the usable limit of the cell's energy content.

4. Temperature Profiling

4.1 Temperature Variations Along the Cell Surface

There are four thermocouples used in measuring thermal conditions in the cell. Three thermocouples are attached to the surface of the cell, and one thermocouple is placed in the vicinity of the thermal chamber. The latter is primarily to ensure that the test temperature provided by the thermal chamber is relatively similar to the desired test temperature. To probe temperature variations along the cell's surface, three thermocouples are fixed close to the negative tab, the positive tab and the centre locations along the surface.

There is a possibility that thermal resistance at the positive tab is higher than at the negative tab. This is reflected by the highest temperature observation at this location at all test temperatures, as shown in Figure 7. Heat generation due to 2-C discharge causes the cell's surface temperature to increase. Although the starting temperature for all thermocouples is relatively identical, the temperature at the positive tab region increases at higher rates when the discharge proceeds. The temperature deviation from the center and negative tab keeps increasing towards the end of discharge. This indicates that additional heat is generated in this region. The additional heat could possibly be in the form of joule heating. When current passes this region, it generates additional heat on top of electrochemical heat. The most significant temperature differences occur at low ambient temperatures. Higher impedance at low temperatures promotes higher heat generation, therefore causing more heat generation while reducing the amount of usable discharge energy. Nevertheless, the general trends remain the same whereby the highest temperature occurs at the positive tab region and it reduces towards the negative tab region.

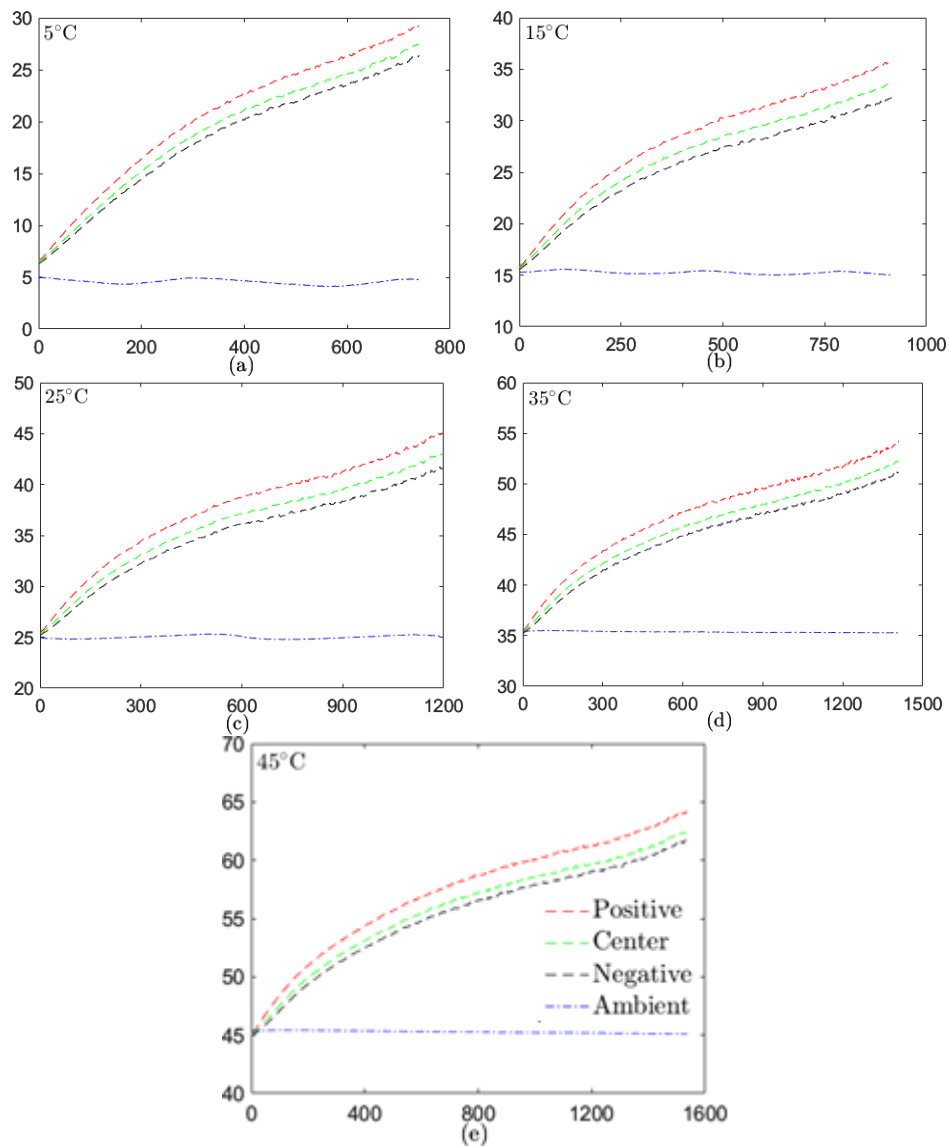


Fig. 7. Temperature profile across cell surface under 2-C full discharge at horizontal arrangement: (a) 5°C ambient, (b) 15°C ambient, (c) 25°C ambient, (d) 35°C ambient and (e) 45°C ambient

4.2 Local Temperature Difference

In order to evaluate the thermal conditions along the cell surface, local temperature analysis is conducted at all test temperatures. Figure 8 compares the dimensional and temporal behaviour of a cell's surface temperature by grouping the temperature profile for each cell's location namely positive, centre and negative region. Higher thermal resistance at the positive tab causes higher peak temperatures in this region. This could contribute by the inherent design of positive tab for cylindrical cell in which it has more component than the negative tab. The tabs design for cylindrical cell are well documented in the public literature and it is relatively similar for all cell manufacturer. Figure 8(a) highlights the temperature increase at the positive region at all test temperatures. As the test temperature gets lower, the final temperature when the cell is at 0% SOC will be the highest.

The highest temperature increase is 22°C, which occurs at 5°C test temperature and this happens at the positive region. The peak temperature reduces moving from centre to negative region with a value of 20°C and 18°C respectively. Surprisingly, the value of temperature increase in all regions, are

relatively similar. Supposedly, the temperature increase at low ambient test temperature should be significantly higher due to higher impedance in this condition. However, as this cell has a smaller thermal mass, the heat generated can exit the cell volume at higher rates. This is also driven by higher temperature differences between the cell's surface and the test temperature or the set temperature of the thermal chamber. Additionally, discharging at higher C-rates shortens the total discharge time, causing the cell to deplete faster. This limits the time for heat to accumulate that eventually reduces the cell's chances of reaching a higher peak temperature. Nevertheless, the trend of higher temperature at positive and it reduces towards negative region can be seen clearly from Figure 8 (left to right). This indicates the thermal resistance plays a role in affecting the temperature profile along the cell surface.

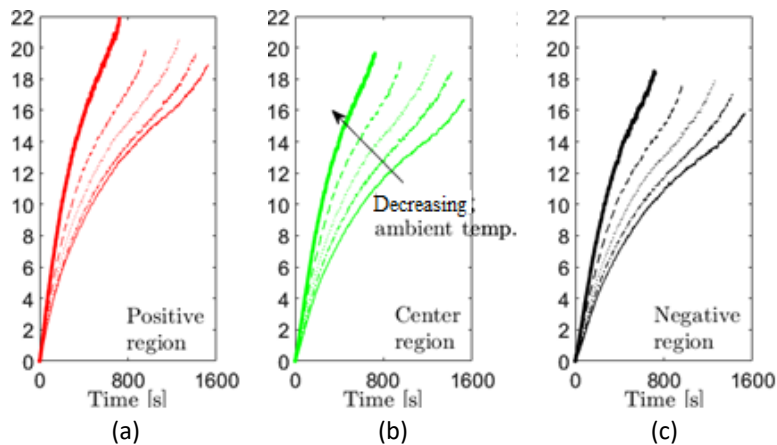


Fig. 8. Temperature difference at three different cell regions at various ambient temperature for cell at horizontal position

Although the peak temperatures at all test temperatures and the cell regions are relatively similar, it is worth noticing that the rate of temperature increase varies significantly. The rate of temperature increase at low ambient temperature testing is consistently higher at all regions. This indicates that heat generation at low temperatures is higher due to a significant increase in cell impedance. Additionally, higher temperature increase rates can be seen towards the end of the discharge as it enters a higher resistance region at low SOC. The condition is exacerbated at low ambient temperatures, where peak temperature can be clearly seen. Temperature data from the start of discharge up to 200 seconds are taken to quantitatively determine the rate of temperature increase at all test temperatures and cell regions. This duration is taken into consideration mainly due to its reasonably linear behaviour. Hence, a temperature differential is conducted to obtain its gradient. Figure 9 illustrates the temperature gradient at all test temperatures and cell regions. The highest rate of temperature increase is approximately $0.05^{\circ}\text{C}/\text{s}$, and it reduces as the test temperature increases. Higher thermal resistance at the positive tab causes additional heat generation, whereby this effect consistently happens along the cell surface. The rate of temperature increase is always higher in the positive tab region, and it reduces in another region. The rate varies significantly with respect to the test temperature; however, the change of rate is relatively constant between positive to negative tab region.

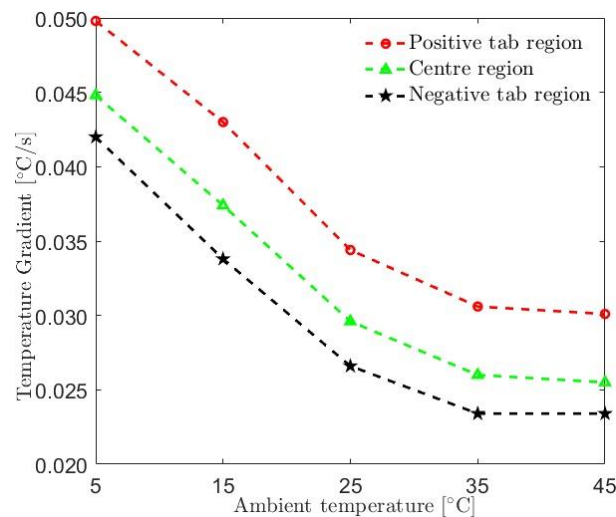


Fig. 9. Rate of temperature increase at early stage of discharge at three different cell regions

5. Energy Evaluation

The same cell is repeatedly used within the specified temperature range and C-rate for this work. These conditions are selected based on the cell manufacturer's specifications. This aims to focus on the cell performance whilst minimising degradation. Since the cell capacity remains unchanged, the energy content of the cell with respect to the applied test temperature and C-rate is evaluated. This parameter is rarely described extensively, mainly because it varies significantly with respect to the test's thermal conditions. The energy content of the cell is evaluated by integrating the voltage curve (Figure 6) at three different C-rate and ambient temperatures and multiplying by the applied current rate. This is mathematically represented by the equation below, and the result is shown in Figure 10.

$$\text{Energy} = I \times \int V dt \text{ (Wh)}$$

A lower C-rate generally causes lower voltage polarization, making more energy available. The energy available at this C-rate is much higher at higher ambient temperatures, as shown in Figure 10. Additionally, since the cell's impedance is lower at high temperatures, more energy is available rather than the energy being converted to thermal energy. This phenomenon can be seen clearly at all C-rates, where more energy is available at a specific C-rate at high ambient test temperatures. Conversely, at lower ambient temperatures, battery electrolyte viscosity increases, leading to higher internal resistance, thus limiting the battery's ability to deliver energy efficiently. From these tests, the maximum energy is 2.3 Wh, which is one order of magnitude difference compared to the worst condition, which is at a 3-C discharge rate at 5°C ambient temperature. These findings highlight the importance of considering ambient temperature and discharge rate for battery optimization.

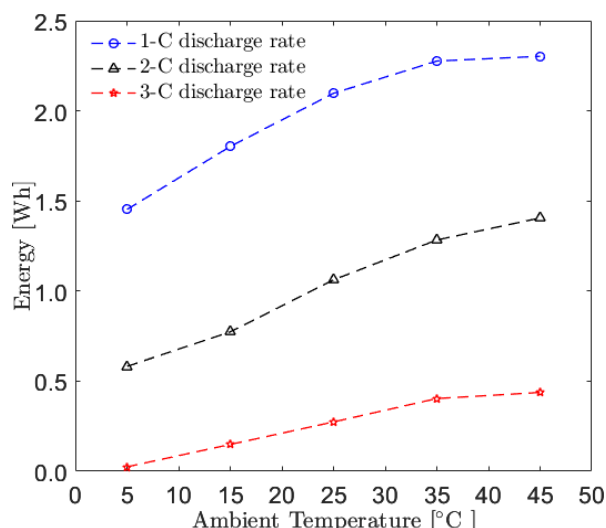


Fig. 10. Energy content at three discharge rates and at various ambient temperature

When examining the battery's behaviour across a spectrum of discharge currents, from high to low, it becomes evident that higher discharge rates often lead to reduced available energy. This is mainly due to a higher rate of voltage polarization, and a significant portion of the cell's energy is converted to thermal energy due to joule heating, which subsequently causes a rapid temperature increase. This analysis could provide insight into energy demand and an understanding of the trade-off between discharge rates and temperature variations. This is crucial to accurately evaluating the energy content of batteries to better facilitate decisions in practical applications and further advancements with regards to battery technology.

6. Conclusions

The presented experimental works aim to establish an understanding of the relationship between thermal conditions and cell performance, focusing on energy and thermal aspects. This work also highlights the presence of a unique temperature profile along the cell surface, which remains consistent across all test temperatures. The maximum temperature difference along the cell surface is approximately 4°C. This could potentially hinder the cell performance due to thermal non-uniformity. It is evident that cell construction has a significant impact on the thermal outcome which is manifested on the cell surface. These findings could assist in the placement of thermal sensors, as they should be positioned at the location with the highest temperature. By examining the cell performance in a broader scale, we can obtain a more precise calculation of the cell's energy content. This departs from the traditional approach, which relies on data from the cell's specification sheet, such as nominal voltage and rated cell capacity.

Acknowledgement

This work was funded by the Universiti Teknologi Malaysia under F4 Grant Scheme (Q.J130000.4624.00Q24).

References

- [1] International Energy Agency. "World Energy Outlook 2020." *IEA*, 2020.
- [2] Ardani, Kristen, Paul Denholm, Trieu Mai, Robert Margolis, Eric O'Shaughnessy, Timothy Silverman, and Jarett Zuboy. "Solar futures study." *US Department of Energy* (2021).

- [3] Abd Aziz, Mohd Azri, Mohd Saifizi Saidon, Muhammad Izuan Fahmi Romli, Siti Marhainis Othman, Wan Azani Mustafa, Mohd Rizal Manan, and Muhammad Zaid Aihsan. "A Review on BLDC Motor Application in Electric Vehicle (EV) using Battery, Supercapacitor and Hybrid Energy Storage System: Efficiency and Future Prospects." *Journal of Advanced Research in Applied Sciences and Engineering Technology* 30, no. 2 (2023): 41-59. <https://doi.org/10.37934/araset.30.2.4159>
- [4] Richardson, Robert R., Shi Zhao, and David A. Howey. "On-board monitoring of 2-D spatially-resolved temperatures in cylindrical lithium-ion batteries: Part I. Low-order thermal modelling." *Journal of Power Sources* 326 (2016): 377-388. <https://doi.org/10.1016/j.jpowsour.2016.06.103>
- [5] Deng, Da. "Li-ion batteries: basics, progress, and challenges." *Energy Science & Engineering* 3, no. 5 (2015): 385-418. <https://doi.org/10.1002/ese3.95>
- [6] Wei, Meng, Palani Balaya, Min Ye, and Ziyong Song. "Remaining useful life prediction for 18650 sodium-ion batteries based on incremental capacity analysis." *Energy* 261 (2022): 125151. <https://doi.org/10.1016/j.energy.2022.125151>
- [7] Hunt, I., T. Zhang, Y. Patel, M. Marinescu, R. Purkayastha, P. Kovacic, S. Walus, A. Swiatek, and G. J. Offer. "The effect of current inhomogeneity on the performance and degradation of Li-S batteries." *Journal of The Electrochemical Society* 165, no. 1 (2017): A6073. <https://doi.org/10.1149/2.0141801jes>
- [8] Ouyang, Dongxu, Jingwen Weng, Mingyi Chen, and Jian Wang. "What a role does the safety vent play in the safety of 18650-size lithium-ion batteries?." *Process Safety and Environmental Protection* 159 (2022): 433-441. <https://doi.org/10.1016/j.psep.2022.01.017>
- [9] Spotnitz, R., and J. Franklin. "Abuse behavior of high-power, lithium-ion cells." *Journal of Power Sources* 113, no. 1 (2003): 81-100. [https://doi.org/10.1016/S0378-7753\(02\)00488-3](https://doi.org/10.1016/S0378-7753(02)00488-3)
- [10] Kong, Depeng, Hengle Zhao, Ping Ping, Yue Zhang, and Gongquan Wang. "Effect of low temperature on thermal runaway and fire behaviors of 18650 lithium-ion battery: A comprehensive experimental study." *Process Safety and Environmental Protection* 174 (2023): 448-459. <https://doi.org/10.1016/j.psep.2023.04.017>
- [11] Hasan, Husam Abdulrasool, Jenan S. Sherza, Jasim M. Mahdi, Hussein Togun, Azher M. Abed, Raed Khalid Ibrahim, and Wahiba Yaïci. "Experimental evaluation of the thermoelectrical performance of photovoltaic-thermal systems with a water-cooled heat sink." *Sustainability* 14, no. 16 (2022): 10231. <https://doi.org/10.3390/su141610231>
- [12] Troxler, Yannic, Billy Wu, Monica Marinescu, Vladimir Yufit, Yatish Patel, Andrew J. Marquis, Nigel P. Brandon, and Gregory J. Offer. "The effect of thermal gradients on the performance of lithium-ion batteries." *Journal of Power Sources* 247 (2014): 1018-1025. <https://doi.org/10.1016/j.jpowsour.2013.06.084>
- [13] Yang, Naixing, Xiongwen Zhang, BinBin Shang, and Guojun Li. "Unbalanced discharging and aging due to temperature differences among the cells in a lithium-ion battery pack with parallel combination." *Journal of Power Sources* 306 (2016): 733-741. <https://doi.org/10.1016/j.jpowsour.2015.12.079>
- [14] Huang, Hsuan-Han, Hsun-Yi Chen, Kuo-Chi Liao, Hong-Tsu Young, Ching-Fei Lee, and Jhen-Yang Tien. "Thermal-electrochemical coupled simulations for cell-to-cell imbalances in lithium-iron-phosphate based battery packs." *Applied Thermal Engineering* 123 (2017): 584-591. <https://doi.org/10.1016/j.applthermaleng.2017.05.105>
- [15] Liu, Xinhua, Weilong Ai, Max Naylor Marlow, Yatish Patel, and Billy Wu. "The effect of cell-to-cell variations and thermal gradients on the performance and degradation of lithium-ion battery packs." *Applied Energy* 248 (2019): 489-499. <https://doi.org/10.1016/j.apenergy.2019.04.108>
- [16] Wang, Qingsong, Qiujuan Sun, Ping Ping, Xuejuan Zhao, Jinhua Sun, and Zijing Lin. "Heat transfer in the dynamic cycling of lithium-titanate batteries." *International Journal of Heat and Mass Transfer* 93 (2016): 896-905. <https://doi.org/10.1016/j.ijheatmasstransfer.2015.11.007>
- [17] Chen, Guangwei, Zhitao Liu, Hongye Su, and Weichao Zhuang. "Electrochemical-distributed thermal coupled model-based state of charge estimation for cylindrical lithium-ion batteries." *Control Engineering Practice* 109 (2021): 104734. <https://doi.org/10.1016/j.conengprac.2021.104734>
- [18] Siddique, Abu Raihan Mohammad, Shohel Mahmud, and Bill Van Heyst. "A comprehensive review on a passive (phase change materials) and an active (thermoelectric cooler) battery thermal management system and their limitations." *Journal of Power Sources* 401 (2018): 224-237. <https://doi.org/10.1016/j.jpowsour.2018.08.094>
- [19] Wang, Qian, Bin Jiang, Bo Li, and Yuying Yan. "A critical review of thermal management models and solutions of lithium-ion batteries for the development of pure electric vehicles." *Renewable and Sustainable Energy Reviews* 64 (2016): 106-128. <https://doi.org/10.1016/j.rser.2016.05.033>
- [20] Xin, Qianqian, Jinsheng Xiao, Tianqi Yang, Hengyun Zhang, and Xi Long. "Thermal management of lithium-ion batteries under high ambient temperature and rapid discharging using composite PCM and liquid cooling." *Applied Thermal Engineering* 210 (2022): 118230. <https://doi.org/10.1016/j.applthermaleng.2022.118230>
- [21] Lyu, Y., A. R. M. Siddique, Shaikh Hasibul Majid, M. Biglarbegian, S. A. Gadsden, and Sahabi Mahmud. "Electric vehicle battery thermal management system with thermoelectric cooling." *Energy Reports* 5 (2019): 822-827. <https://doi.org/10.1016/j.egyr.2019.06.016>

- [22] Nasir, Faiza Mohamed, Mohd Zulkifly Abdullah, and Mohd Azmi Ismail. "Effect of Heat Pipe's Configuration in Managing the Temperature of EV Battery." *CFD Letters* 15, no. 3 (2023): 22-34. <https://doi.org/10.37934/cfdl.15.3.2234>
- [23] Shetty, Divya D., Mahamad Sulthan, Mohammad Zuber, Irfan Anjum Badruddin, and Chandrakant R. Kini. "Computational design and analysis of a novel battery thermal management system of a single 26650 Li-ion battery cell for electric vehicle application." *Journal of Advanced Research in Fluid Mechanics and Thermal Sciences* 93, no. 2 (2022): 61-75. <https://doi.org/10.37934/arfmts.93.2.6175>
- [24] Fan, Ruijin, Nianben Zheng, and Zhiqiang Sun. "Evaluation of fin intensified phase change material systems for thermal management of Li-ion battery modules." *International Journal of Heat and Mass Transfer* 166 (2021): 120753. <https://doi.org/10.1016/j.ijheatmasstransfer.2020.120753>
- [25] Kumar, Rajat, and Varun Goel. "A study on thermal management system of lithium-ion batteries for electrical vehicles: A critical review." *Journal of Energy Storage* 71 (2023): 108025. <https://doi.org/10.1016/j.est.2023.108025>
- [26] Tian, Man-Wen, Azher M. Abed, Shu-Rong Yan, S. Mohammad Sajadi, Mustafa Z. Mahmoud, Hikmet S. Aybar, and Ghassan Fadhil Smaism. "Economic cost and numerical evaluation of cooling of a cylindrical lithium-ion battery pack using air and phase change materials." *Journal of Energy Storage* 52 (2022): 104925. <https://doi.org/10.1016/j.est.2022.104925>
- [27] Wang, Chun, Huan Xi, and Meiwei Wang. "Investigation on forced air-cooling strategy of battery thermal management system considering the inconsistency of battery cells." *Applied Thermal Engineering* 214 (2022): 118841. <https://doi.org/10.1016/j.applthermaleng.2022.118841>
- [28] Yang, Ruoyu, Meiwei Wang, and Huan Xi. "Thermal investigation and forced air-cooling strategy of battery thermal management system considering temperature non-uniformity of battery pack." *Applied Thermal Engineering* 219 (2023): 119566. <https://doi.org/10.1016/j.applthermaleng.2022.119566>
- [29] Lu, Hao, and Xiaole Tang. "A flexible optimization study on air-cooled battery thermal management system by considering of system volume and cooling performance." *Journal of Energy Storage* 72 (2023): 108527. <https://doi.org/10.1016/j.est.2023.108527>
- [30] Liu, Yuanzhi, and Jie Zhang. "Design a J-type air-based battery thermal management system through surrogate-based optimization." *Applied Energy* 252 (2019): 113426. <https://doi.org/10.1016/j.apenergy.2019.113426>
- [31] Akbarzadeh, Mohsen, Theodoros Kalogiannis, Lu Jin, Danial Karimi, Joeri Van Mierlo, and Maitane Berecibar. "Experimental and numerical thermal analysis of a lithium-ion battery module based on a novel liquid cooling plate embedded with phase change material." *Journal of Energy Storage* 50 (2022): 104673. <https://doi.org/10.1016/j.est.2022.104673>
- [32] Hong, Seong Ho, Dong Soo Jang, Seonggi Park, Sungho Yun, and Yongchan Kim. "Thermal performance of direct two-phase refrigerant cooling for lithium-ion batteries in electric vehicles." *Applied Thermal Engineering* 173 (2020): 115213. <https://doi.org/10.1016/j.applthermaleng.2020.115213>
- [33] Hales, Alastair, Laura Bravo Diaz, Mohamed Waseem Marzook, Yan Zhao, Yatish Patel, and Gregory Offer. "The cell cooling coefficient: A standard to define heat rejection from lithium-ion batteries." *Journal of The Electrochemical Society* 166, no. 12 (2019): A2383-A2395. <https://doi.org/10.1149/2.0191912jes>